Research Square

Preprints are preliminary reports that have not undergone peer review.
They should not be considered conclusive, used to inform clinical practice,
or referenced by the media as validated information.

Early life stages for juvenile sporophytes of a sub-Antarctic giant kelp under glacier-retreat associated changes: interactive effects of salinity and irradiance in Macrocystis pyrifera (Phaeophyceae)

Camila Gómez-Mardones
Laboratory of Antarctic and Sub-Antarctic Marine Ecosystems (LEMAS)
Johanna Marambio
Laboratory of Antarctic and Sub-Antarctic Marine Ecosystems (LEMAS)
Juan Pablo Olivos
juolivos@umagallanes.cl
Laboratory of Antarctic and Sub-Antarctic Marine Ecosystems (LEMAS)
Francisco Bahamonde
Laboratory of Antarctic and Sub-Antarctic Marine Ecosystems (LEMAS)
Juan Pablo Rodríguez
Laboratory of Antarctic and Sub-Antarctic Marine Ecosystems (LEMAS)
Andrés Mansilla
Laboratory of Antarctic and Sub-Antarctic Marine Ecosystems (LEMAS)

Research Article

Keywords: Climate change, Glacial meltwater, Hyposalinity, Macrocystis pyrifera, Magellanic Sub-Antarctic Ecoregion

Posted Date: November 23rd, 2026

DOI: https://doi.org/10.21203/rs.3.rs-11692362/v1

License: This work is licensed under a Creative Commons Attribution 4.0 International License.
Read Full License

Additional Declarations: No competing interests reported.

Early life stages for juvenile sporophytes of a sub-Antarctic giant kelp under glacier-retreat associated changes: interactive effects of salinity and irradiance in *Macrocystis pyrifera* (Phaeophyceae)

Camila Gómez-Mardones[1,2,3,5], Johanna Marambio[1,3], Juan Pablo Olivos[1,2,3], Francisco Bahamonde[1, 3, 4, 5], Juan Pablo Rodríguez[1,3,4], Andrés Mansilla[1,3]

[1] Laboratory of Antarctic and Sub-Antarctic Marine Ecosystems (LEMAS), University of Magallanes, Punta Arenas, Chile.
[2] Master's Program in Sciences, specializing in Management and Conservation of Natural Resources in Subantarctic Environments, University of Magallanes, Punta Arenas, Chile.
[3] Cape Horn International Center (CHIC), University of Magallanes, Puerto Williams, Chile.
[4] Doctoral Program in Antarctic and Subantarctic Sciences, University of Magallanes, Punta Arenas, Chile.
[5] Millennium Institute Biodiversity of Antarctic and Subantarctic Ecosystems (BASE), University of Chile, Santiago, Chile.

Corresponding author: Juan Pablo Olivos
E-mail: juolivos@umagallanes.cl

Abstract

Glacier retreat associated with climate change is simultaneously altering salinity and light availability in coastal ecosystems of the Magellanic Sub-Antarctic Ecoregion. However, the combined effects of these factors on the early life stages of *Macrocystis pyrifera* remain poorly understood. In this study, we evaluated the growth and photosynthetic performance of juvenile sporophytes cultured from reproductive material collected in the Strait of Magellan. Juveniles were exposed for 21 days to a factorial combination of three salinities (12, 21, and 30 g kg^{-1}) and three irradiances (5, 10, and 17 µmol photons m^{-2} s^{-1}). Relative area growth rate was affected by salinity, irradiance, and their interaction, whereas biomass growth responded independently to salinity and irradiance. Overall, growth declined under hyposalinity and low irradiance. The maximum quantum yield of photosystem II (F_v/F_m) and the maximum relative electron transport rate ($rETR_{max}$) also showed an interaction between salinity and irradiance, with the lowest values occurring under hyposalinity and intermediate irradiance. Final F_v/F_m values ranged from 0.519 ± 0.03 to 0.731 ± 0.02 (mean ± SD). These results suggest that hyposalinity modifies the response of juvenile sporophytes to light availability and suggest a potential vulnerability of early developmental stages to environmental changes associated with glacier retreat. Because these stages underpin recruitment and population renewal, their sensitivity may pose a risk to the recovery capacity and persistence of sub-Antarctic kelp forests.

Keywords: Climate change; Glacial meltwater; Hyposalinity; *Macrocystis pyrifera*; Magellanic Sub-Antarctic Ecoregion.

Acknowledgments

We gratefully acknowledge funding from FONDECYT Regular project No. 1241697, the Cape Horn International Center (CHIC) Project ANID/BASAL FB210018, and PROASA Project 2025/07548-9. The authors also wish to thank the Laboratory of Antarctic and Sub-Antarctic Marine Ecosystems (LEMAS), Universidad de Magallanes, for providing technical support and laboratory facilities.

Introduction

The Magellanic Sub-Antarctic Ecoregion, situated between 47° and 56°S and 71° and 73°W (Fig. 1), constitutes one of the largest and most environmentally heterogeneous marine regions in the Southern Hemisphere (Marambio et al. 2023; Rosenfeld et al. 2023; Ojeda et al. 2026). This region is characterized by a complex network of fjords, channels, archipelagos, and islands, whose present-day configuration reflects glacial and postglacial processes (Rivera et al. 2023). In these high-latitude environments, interactions among coastal geomorphology, strong westerly winds, freshwater inputs from precipitation, rivers, and glaciers, and pronounced seasonality generate substantial environmental heterogeneity (Bahamonde et al. 2022). Consequently, variables such as salinity, temperature, turbidity, and light availability exhibit considerable spatial and temporal variability, influencing the structure and functioning of coastal communities and the performance of photosynthetic organisms (Bahamonde et al. 2024). This heterogeneity, occurring over relatively short geographic distances, makes the Magellanic Sub-Antarctic Ecoregion a natural laboratory for studying the responses of marine ecosystems to climate change (Rozzi et al. 2012). In this context, macroalgal communities provide a particularly relevant model for understanding how environmental variability and ongoing environmental change can propagate from organismal physiological responses to the functioning of coastal ecosystems.

Within these environments, kelp forests are among the most important structural and functional components of coastal ecosystems. These macroalgae act as foundation species and ecosystem engineers, providing habitat, refuge, and food for a wide diversity of marine organisms, while also contributing substantially to primary productivity and energy flow (Marambio et al. 2023; Rodríguez et al. 2026). Among the species forming these forests, *Macrocystis pyrifera* is widely distributed across temperate and subpolar regions of both hemispheres (Gonzalez-Aragon et al. 2024; Ojeda et al. 2026). In Chile, its distribution extends from approximately -30° S to -56° S (Marambio et al. 2023; Gonzalez-Aragon et al. 2024), becoming particularly dominant in the Sub-Antarctic region of southernmost South America. There, its extensive underwater forests provide important ecosystem functions and services through their high productivity and capacity to modify the physical and biological conditions of the surrounding habitat (Marambio et al. 2023; Ojeda et al. 2026).

Over recent decades, climate change has accelerated glacier retreat in southern South America, increasing freshwater, sediment, and particulate matter inputs into coastal ecosystems (Dussaillant et al. 2019; Coral-Santacruz et al. 2024). In an ecoregion where numerous *M. pyrifera* forests occur in fjords and channels under the direct or indirect influence of glacial systems, these changes can lead to hyposaline conditions in surface waters and increased turbidity, while simultaneously altering the availability of photosynthetically active radiation (PAR) throughout the water column (Coral-Santacruz et al. 2024). Consequently, macroalgae inhabiting glacier-influenced environments are

simultaneously exposed to variations in osmotic conditions and light availability for photosynthesis (Lebrun et al. 2024).

Irradiance and salinity are important regulators of macroalgal metabolism and physiological performance. Light availability directly influences photosynthetic activity and can affect photochemical efficiency and electron transport (Marambio et al. 2022a). In response to the high variability in light conditions characteristic of high-latitude environments, *M. pyrifera* exhibits photoacclimation mechanisms that include changes in the composition and concentration of photosynthetic pigments and adjustments in energy dissipation mechanisms, allowing it to maintain photosynthetic performance under different light regimes (Marambio et al. 2017; Coral-Santacruz et al. 2024). In contrast, hyposalinity can induce osmotic and ionic imbalances, potentially compromising photosynthesis and growth (Marambio et al. 2022b; Rodríguez et al. 2026).

These effects are particularly critical during the early life stages of *M. pyrifera*, potentially affecting spore germination, gametophyte development, and the establishment of juvenile sporophytes (Rodríguez et al. 2019; Coral-Santacruz et al. 2024). This sensitivity is particularly relevant from an ecological perspective, as success during early developmental stages is critical for the recruitment, renewal, and persistence of *M. pyrifera* forests (Barrientos et al. 2024). Several studies conducted in southern Chile have documented the ecophysiological responses of this species to environmental factors such as irradiance, temperature, and salinity (Marambio et al. 2017; Coral-Santacruz et al. 2024; Rodríguez et al. 2026). However, most of these studies have examined these factors independently, whereas their interactive effects during early life stages remain less understood. This knowledge gap is particularly relevant in the Magellanic Sub-Antarctic Ecoregion, where glacier retreat can simultaneously alter multiple habitat characteristics. Experimentally evaluating the interaction between these factors provides a more realistic representation of the conditions experienced by natural populations and can improve our understanding of how their physiological responses may influence the capacity for renewal of *M. pyrifera* forests under environmental changes associated with climate change.

In this context, the aim of this study was to evaluate the individual and combined effects of salinity and irradiance on growth, expressed as changes in area and biomass, and on the photosynthetic performance of juvenile *M. pyrifera* sporophytes cultured under controlled laboratory conditions. We hypothesized that hyposalinity would affect the physiological performance of juvenile sporophytes and modify their response to light availability. Accordingly, we predicted that the effects of irradiance on photosynthetic performance and growth would vary depending on salinity conditions, with stronger negative effects under hyposalinity.

Materials and Methods

Study area

Fertile fronds of *M. pyrifera* were manually collected on 18 June 2025 at Punta Santa Ana (53°37′ S, 70°52′ W; Brunswick Peninsula, Strait of Magellan, Chile; Fig. 1), located in the central microbasin of the strait within the Magellanic Sub-Antarctic Ecoregion. This microbasin is characterized by

modified Sub-Antarctic waters, with a mean salinity of 30.8 and temperatures of ~7 °C (Valdenegro and Silva 2003; Marambio et al. 2017). Fronds were transported to the Laboratory of Antarctic and Sub-Antarctic Marine Ecosystems (LEMAS), Universidad de Magallanes, for processing and cultivation.

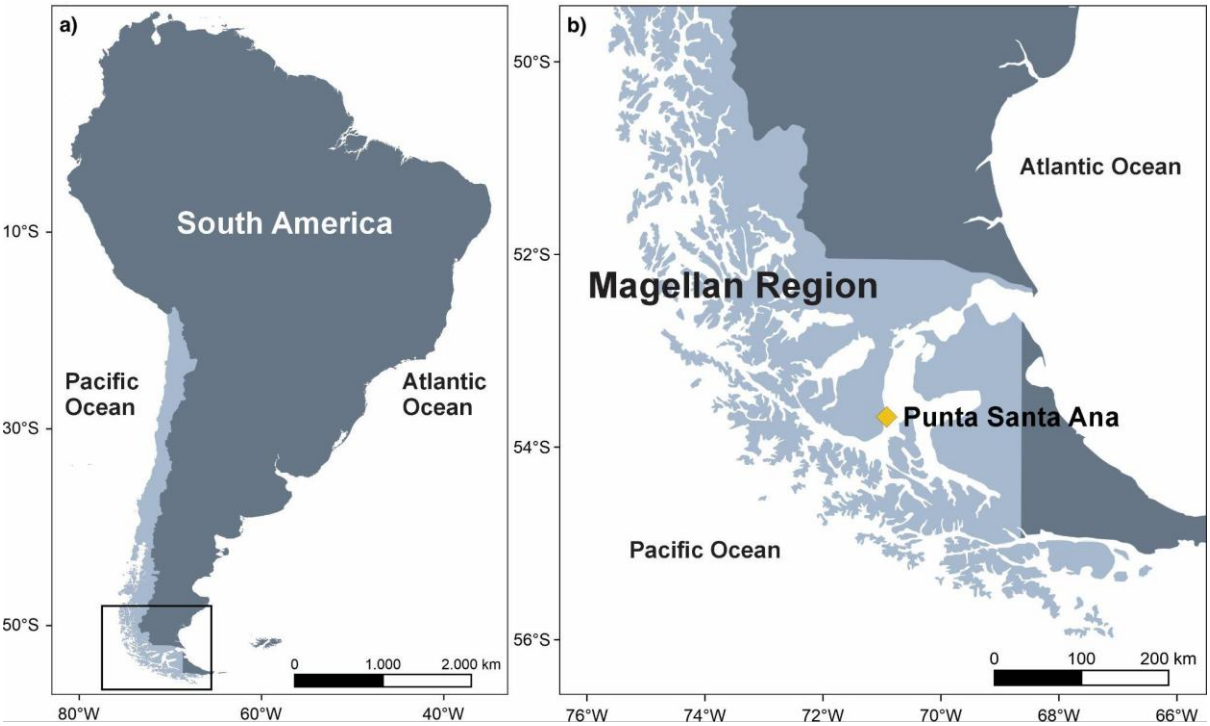

Fig. 1 Location of the *M. pyrifera* collection site at Punta Santa Ana, Magallanes and Chilean Antarctic Region, Chile. (a) Location of the Magallanes Region in southern South America. (b) Location of Punta Santa Ana in the Strait of Magellan.

Obtaining and culturing juvenile sporophytes

Juvenile sporophytes used in the experiments were obtained from zoospores released from fertile sporophylls of *M. pyrifera* collected at Punta Santa Ana, following previously described protocols for the species (Ávila et al. 2010; Le et al. 2022). Sporophylls were washed with freshwater to remove epibionts and particulate matter and subsequently rinsed three times with filtered (0.45 µm) and sterilized seawater. They were then blotted dry with absorbent paper and incubated in darkness for 12 h at 8 °C to induce zoospore release (Ávila et al. 2010). Sporophyll fragments were subsequently rehydrated in filtered seawater enriched with Provasoli Enriched Seawater medium (PES; McLachlan 1973) to promote zoospore release.

Cultures were maintained in filtered seawater supplemented with PES medium (10 mL L^{-1}) under controlled conditions of temperature (9°C), a 12 h light:12 h dark photoperiod, and an irradiance of 10 µmol photons m^{-2} s^{-1} (Ávila et al. 2010; Le et al. 2022). The culture medium was renewed twice weekly to maintain adequate nutrient availability and stable conditions throughout the development of the different life-cycle stages. Microscopic development was monitored weekly using a light microscope. Differentiated gametophytes were observed approximately 19 days after zoospore release, whereas the first juvenile sporophytes were recorded approximately 56 days after seeding.

Juvenile sporophytes were subsequently maintained in culture for approximately five months at a salinity of 30 g kg^{-1} and under the same temperature, irradiance, and photoperiod conditions described above, until they reached a suitable size for the experiments. The sporophytes obtained from these cultures constituted the biological material used in all experimental treatments.

Experimental design

The experiment was conducted for 21 days under controlled laboratory conditions using a completely randomized 3 × 3 factorial design (Fig. 2). Three salinity levels (S: SA12 = 12 g kg^{-1}, SA21 = 21 g kg^{-1}, and SA30 = 30 g kg^{-1}) and three irradiance levels (I: low light, LL = 5 µmol photons m^{-2} s^{-1}; medium light, ML = 10 µmol photons m^{-2} s^{-1}; and high light, HL = 17 µmol photons m^{-2} s^{-1}) were evaluated, resulting in nine treatments with three independent replicates per treatment (n = 3; 27 experimental units in total). All experimental units were maintained within a single temperature-controlled chamber. Irradiance levels were established by adjusting the distance between the LED lamps and the culture flasks and were measured and verified at flask height using an RBRsolo³ PAR photosynthetically active radiation logger (RBR Ltd., Ottawa, Canada).

Salinity treatments were prepared by diluting seawater with distilled water to obtain the target salinities of 12, 21, and 30 g kg^{-1}. Salinity was adjusted and verified using a handheld refractometer (ATAGO S-10E, Japan), and the culture medium was subsequently supplemented with Provasoli Enriched Seawater (PES; 10 mL L^{-1}). Juvenile sporophytes previously maintained at 30 g kg^{-1} were gradually acclimated to their assigned salinity treatments. Each experimental unit consisted of a 500-mL flask containing an initial wet biomass of 0.5 g of randomly selected juvenile sporophytes, corresponding to approximately 51 ± 19.92 individuals per flask (mean ± SD). Before the application of salinity and irradiance treatments, the initial F_v/F_m was measured in three samples (day 0), establishing a common baseline of 0.712 ± 0.02 (mean ± SD, n = 3) for all experimental conditions.

The culture medium was renewed twice weekly, and the flasks were randomly repositioned within their corresponding irradiance zone at each medium renewal to minimize potential positional effects. Throughout the 21-day experiment, temperature was maintained at 9 °C, a 12 h light:12 h dark photoperiod was applied, and continuous gentle aeration was provided using an aquarium air pump (HAILEA ACO-9905, Guangdong Hailea Group Co., Ltd., China) (Fig. 2). The salinity levels represented a gradient of hyposalinity associated with freshwater inputs in the Magellanic Sub-Antarctic Ecoregion: SA30 was used as a reference for salinity conditions in the Strait of Magellan (Valdenegro and Silva 2003; Frangopulos et al. 2026), SA21 represented an intermediate condition, and SA12 represented a more intense hyposaline condition. HL and ML fell within the irradiance range used during pre-experimental culture (10–20 µmol photons m^{-2} s^{-1}), whereas LL (5 µmol photons m^{-2} s^{-1}) was below it; together, these levels represented a gradient of light limitation, simulating reduced light availability due to glacier-retreat-associated turbidity (Coral-Santacruz et al. 2024; Rodríguez et al. 2026).

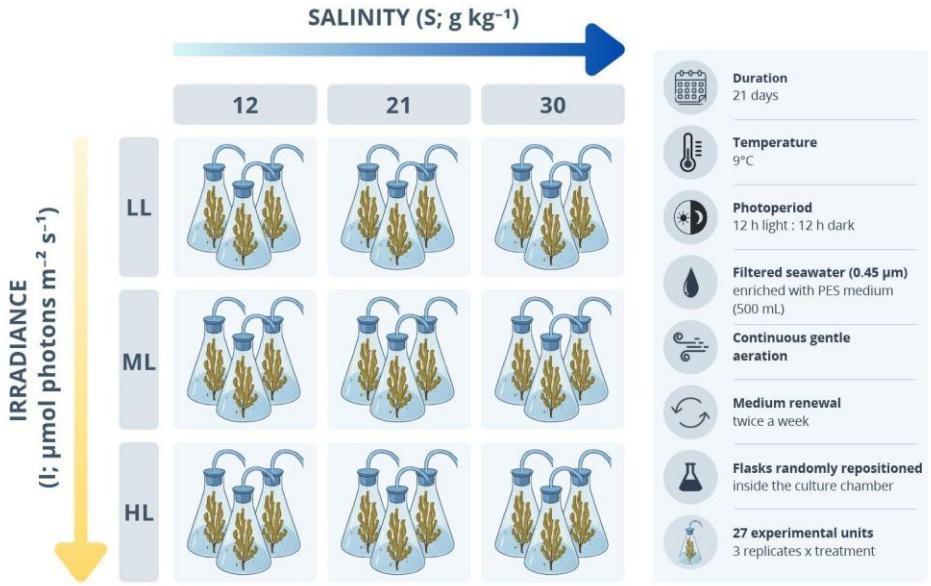

Fig. 2 Experimental design used to evaluate the effects of three salinity levels (SA12, SA21, and SA30 g kg^{-1}) and three irradiance levels (LL = 5, ML = 10, and HL = 17 µmol photons m^{-2} s^{-1}) on juvenile *M. pyrifera* sporophytes over 21 days.

Physiological responses

Area growth

Area growth was quantified through digital analysis of photographs obtained during the experiment (days 0, 7, 14, and 21). Photographs were analyzed using ImageJ software to determine the projected area of each sporophyte (mm^2). Individual areas were summed to obtain the total sporophyte area within each experimental unit. To assess temporal changes in growth, relative area (%) was calculated with respect to the initial area of each experimental unit. Additionally, the relative growth rate in area (RGR_{area}; % day^{-1}) was calculated following Yong et al. (2013):

$$RGR_{area} = ln\left(\frac{A_t}{A_0}\right) t^{-1} \times 100$$

where A_0 and A_t represent the total sporophyte area (mm^2) within each experimental unit at the beginning and end of the experiment, respectively, and t is the elapsed time (days).

Biomass growth

Total wet biomass of the sporophytes within each experimental unit was measured at the beginning and end of the experiment using a RADWAG AS 220/C/2 analytical balance (RADWAG, Poland). Prior to weighing, excess surface water was removed using absorbent paper to minimize its contribution to wet biomass measurements. The relative growth rate in biomass ($RGR_{biomass}$; % day^{-1}) was calculated following Yong et al. (2013):

$$RGR_{biomass} = ln\left(\frac{B_f}{B_i}\right) t^{-1} \times 100$$

where B_i and B_f represent the total wet biomass (g) within each experimental unit at the beginning and end of the experiment, respectively, and t is the elapsed time (days).

Photosynthetic response

The photosynthetic response of *M. pyrifera* was assessed using pulse-amplitude-modulated (PAM) fluorometry with a Mini-PAM II fluorometer (Walz, Effeltrich, Germany). For each measurement, one juvenile sporophyte was randomly selected from each experimental unit. Prior to each measurement, samples were dark-adapted for 6 min. After fluorescence measurements, each sporophyte was returned to its respective culture flask. The maximum quantum yield of photosystem II (F_v/F_m) was measured before the application of experimental treatments (day 0) and subsequently on days 14 and 21. On day 21, PAM measurements were performed after the final photographs and biomass measurements had been obtained. The initial measurements (n = 3) established a common baseline, whereas measurements on days 14 and 21 were obtained from each experimental unit to characterize photosynthetic responses under the different treatments.

Additionally, rapid light curves (RLCs) were obtained by sequentially exposing samples to 13 levels of actinic irradiance, ranging from 0 to 1500 µmol photons m^{-2} s^{-1}, using the same fluorometer. Each actinic irradiance step lasted 20 s. Fluorescence measurements were performed using a measuring light intensity of 1, a saturation pulse intensity of 10 with a duration of 0.6 s, a gain of 2, and a damping setting of 2.

The relative electron transport rate (rETR) at each irradiance step was calculated as:

$$rETR = PAR \times Y(II)$$

where PAR is the applied actinic irradiance (µmol photons m^{-2} s^{-1}) and Y(II) is the effective quantum yield of PSII ($\Delta F/F_m'$). Because the calculation does not incorporate sample absorptance or the fraction of absorbed light allocated to PSII, electron transport was expressed as a relative rate (rETR).

The following photosynthetic parameters were estimated from the rETR–irradiance curves: maximum relative electron transport rate ($rETR_{max}$), defined as the maximum value estimated from the fitted curves; initial slope (α), representing the initial slope of the rETR–irradiance relationship; and light saturation point (E_k), calculated as the ratio $rETR_{max}/\alpha$ and expressed as µmol photons m^{-2} s^{-1}. These parameters were obtained by fitting the rETR–irradiance data to the nonlinear model of Platt et al. (1980), implemented in KaleidaGraph v4.0 (Synergy Software, Reading, PA, USA). Maximum quantum yield was calculated as $F_v/F_m = (F_m - F_0)/F_m$, where F_m represents the maximum fluorescence measured after the saturation pulse and F_0 the minimum fluorescence measured in the dark-adapted state.

Statistical analyses

Prior to statistical analyses, residual normality and homogeneity of variances were assessed using the Shapiro–Wilk and Levene tests, respectively. RGR_{area}, $RGR_{biomass}$, F_v/F_m, $rETR_{max}$, α, and E_k were analyzed using two-way analysis of variance (ANOVA), with salinity (S), irradiance (I), and their interaction (S × I) included as fixed effects. Factorial models were fitted using the *lm()* function in R, and Type III ANOVA tables were obtained using the *car* package with sum-to-zero contrasts. When appropriate, pairwise comparisons were performed using Tukey-adjusted estimated marginal means calculated with the *emmeans* package. For F_v/F_m, $rETR_{max}$, E_k, and α, inferential analyses were restricted to day 21 to assess treatment effects after 21 days of exposure, whereas measurements at days 0 and 14 were used to descriptively characterize temporal variation. Significance group letters were generated using the *multcomp* and *multcompView* packages. Data processing and graphical representations were performed using *dplyr* and *ggplot2*. All statistical analyses were conducted in R version 4.2.2 (R Core Team 2022), using a significance level of $p < 0.05$.

Results

Growth

Area growth

RGR_{area} was significantly affected by salinity ($F_{2,18} = 73.31$, $p < 0.001$), irradiance ($F_{2,18} = 58.75$, $p < 0.001$), and their interaction ($F_{4,18} = 3.58$, $p = 0.026$; Fig. 3; Online Resource 2). Overall, growth increased with salinity, while, within each salinity level, significantly higher growth rates were observed under ML and HL compared with LL. The highest values were recorded at SA30 under ML (7.72 ± 1.13% day^{-1}) and HL (7.70 ± 0.74% day^{-1}), whereas the lowest growth was observed at SA12 under LL (1.45 ± 0.28% day^{-1}) (Fig. 3; Online Resource 1).

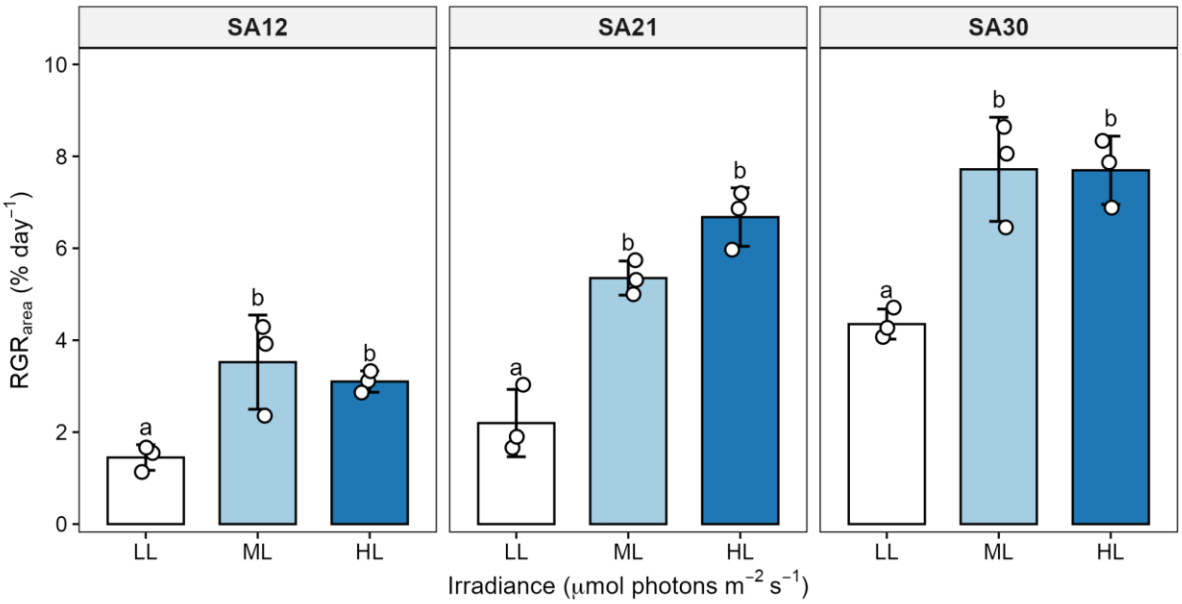

Fig. 3 RGR_{area} of juvenile *M. pyrifera* sporophytes exposed to three salinity levels (SA12, SA21, and SA30 g kg^{-1}) and three irradiance levels (LL = 5, ML = 10, and HL = 17 µmol photons m^{-2} s^{-1}) over 21 days. Bars represent mean values, error bars indicate standard deviation (SD), and points represent

individual independent replicates (n = 3 per treatment). Different lowercase letters indicate significant differences among irradiance levels within each salinity level according to Tukey's post hoc test (p < 0.05)

Biomass growth

$RGR_{biomass}$ was significantly affected by salinity ($F_{2,18}$ = 3.82, p = 0.041) and irradiance ($F_{2,18}$ = 7.63, p = 0.004), whereas no significant interaction between these factors was detected ($F_{4,18}$ = 1.67, p = 0.200; Fig. 4; Online Resource 3). Overall, $RGR_{biomass}$ tended to increase with salinity, with significantly higher values at SA30 than at SA12. Similarly, when averaged across salinity levels, ML and HL resulted in significantly higher growth rates than LL. The highest mean growth was recorded at SA30 under HL (8.95 ± 1.81% day^{-1}), whereas the lowest was observed at SA12 under LL (3.95 ± 1.95% day^{-1}) (Fig. 4; Online Resource 1).

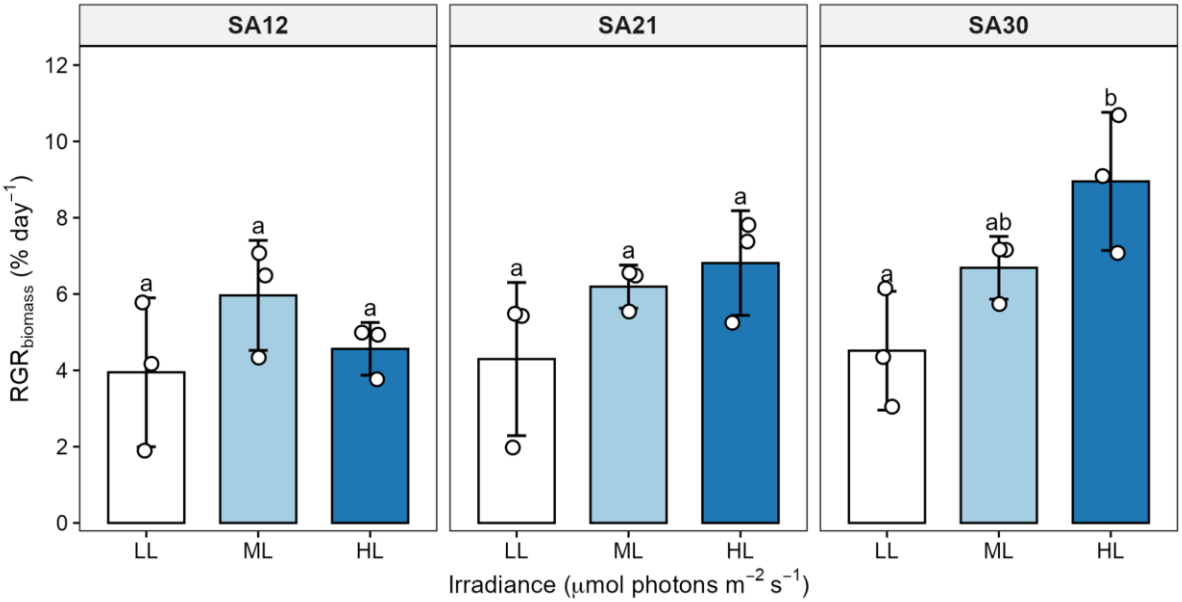

Fig. 4 $RGR_{biomass}$ of juvenile *M. pyrifera* sporophytes exposed to three salinity levels (SA12, SA21, and SA30 g kg^{-1}) and three irradiance levels (LL = 5, ML = 10, and HL = 17 μmol photons m^{-2} s^{-1}) over 21 days. Bars represent mean values, error bars indicate standard deviation (SD), and points represent individual independent replicates (n = 3 per treatment). Different lowercase letters indicate significant differences among irradiance treatments within each salinity level according to Tukey's post hoc test (p < 0.05)

Photosynthetic response

Maximum quantum yield of photosystem II (F_v/F_m)

F_v/F_m was significantly affected by salinity ($F_{2,18}$ = 7.73, p = 0.004), irradiance ($F_{2,18}$= 26.60, p < 0.001), and their interaction ($F_{4,18}$ = 2.97, p = 0.048; Fig. 5; Online Resource 4). At SA12 and SA21, F_v/F_m values were significantly lower under ML than under LL and HL, whereas no significant differences among irradiance levels were detected at SA30. The highest final F_v/F_m value was recorded

at SA30 under LL (0.731 ± 0.02; Fig. 5), whereas the lowest was observed at SA12 under ML (0.519 ± 0.03; Fig. 5; Online Resource 1).

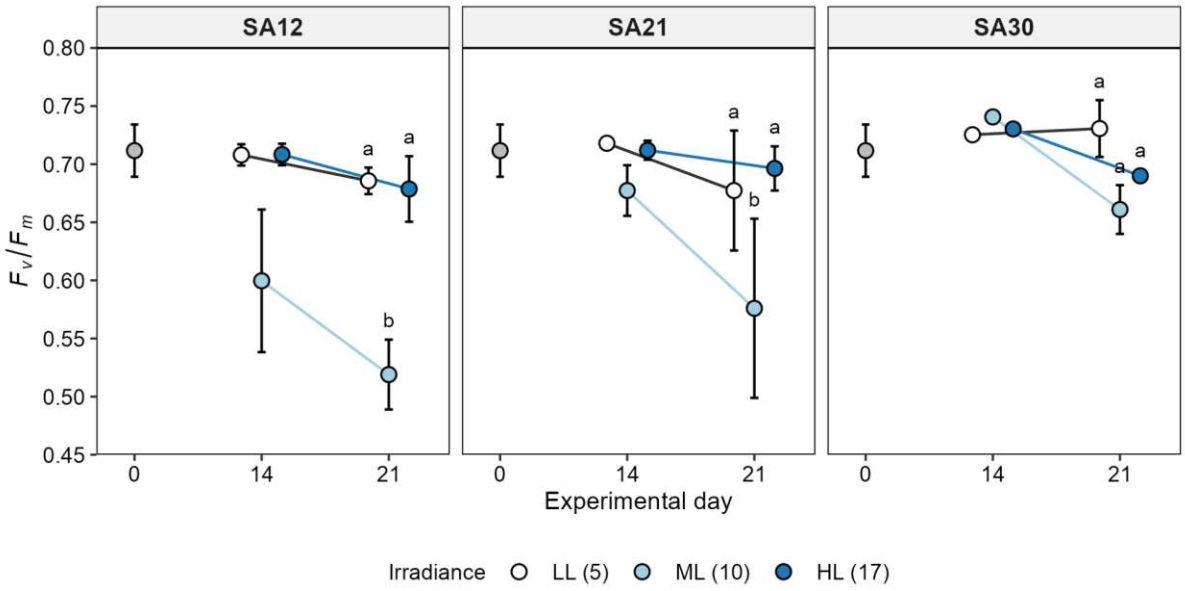

Fig. 5 Temporal variation in F_v/F_m of juvenile *M. pyrifera* sporophytes exposed to three salinity levels (SA12, SA21, and SA30 g kg^{-1}) and three irradiance levels (LL = 5, ML = 10, and HL = 17 µmol photons m^{-2} s^{-1}). Symbols represent mean values and error bars indicate standard deviation (SD; n = 3). Day 0 represents a common baseline displayed in all three panels, while lines connect treatment means between days 14 and 21. Different lowercase letters indicate significant differences among irradiance treatments within each salinity level at day 21 (Tukey's post hoc test, $p < 0.05$)

Photosynthetic parameters

$rETR_{max}$ was significantly affected by irradiance ($F_{2,18}$= 14.31, $p < 0.001$) and the salinity × irradiance interaction ($F_{4,18}$= 3.85, $p = 0.020$), whereas no significant effect of salinity was detected ($F_{2,18} = 2.76$, $p = 0.090$) (Table 1; Online Resource 5). At SA12, $rETR_{max}$ was significantly lower under ML than under LL and HL, reaching a minimum of 10.47 ± 2.90 (rel. units). At SA21, $rETR_{max}$ was significantly lower under ML than under HL ($p = 0.0473$; Online Resource 5), whereas no significant differences among irradiance levels were detected at SA30. The highest final $rETR_{max}$ value was recorded at SA12 under LL (27.96 ± 4.89 rel. units).

For α, ANOVA showed a significant main effect of irradiance ($F_{2,18} = 19.74$, $p < 0.001$), whereas salinity ($F_{2,18} = 0.72$, $p = 0.499$) and the salinity × irradiance interaction ($F_{4,18} = 1.64$, $p = 0.208$) showed no significant effects (Table 1; Online Resource 6). Tukey's post hoc comparisons indicated that α was significantly lower under ML than under LL and HL when averaged across salinity levels ($p < 0.001$), with no significant difference detected between LL and HL ($p = 0.980$; Online Resource 6). The highest mean value was recorded at SA12 under LL (0.288 ± 0.05), whereas the lowest was observed at SA12 under ML (0.201 ± 0.02; Table 1).

E_k was significantly affected by irradiance ($F_{2,18}$ = 3.75, p = 0.043) and the salinity × irradiance interaction ($F_{4,18}$ = 2.96, p = 0.049), whereas no significant effect of salinity was detected ($F_{2,18}$ = 2.69, p = 0.095; Table 1; Online Resource 7). However, Tukey's post hoc comparisons revealed no significant differences among the evaluated treatment pairs (p > 0.05; Online Resource 7). The highest E_k value was recorded at SA30 under LL (107.822 ± 25.50 µmol photons m^{-2} s^{-1}), whereas the lowest was observed at SA21 under LL (48.401 ± 9.53 µmol photons m^{-2} s^{-1}; Table 1).

Table 1 Photosynthetic parameters ($rETR_{max}$, α, and E_k) of juvenile *M. pyrifera* sporophytes exposed to three salinity levels (SA12, SA21, and SA30, corresponding to 12, 21, and 30 g kg^{-1}, respectively) and three irradiance levels (LL = 5, ML = 10, and HL = 17 µmol photons m^{-2} s^{-1}) for 21 days. Values are presented as mean ± standard deviation (SD; n = 3). The final three rows show p-values from two-way ANOVA for salinity (S), irradiance (I), and their interaction (S × I). Significant effects (p < 0.05) are indicated in bold. N/A indicates not applicable. Detailed ANOVA results and Tukey-adjusted pairwise comparisons are provided in Online Resources 5–7.

Salinity	Irradiance	$rETR_{max}$ (rel. units)	α	E_k (µmol photons m^{-2} s^{-1})
	LL	27.958 (± 4.89)	0.288 (± 0.05)	104.414 (± 33.04)
SA12	ML	10.465 (± 2.90)	0.201 (± 0.02)	49.407 (± 10.23)
	HL	25.689 (± 6.00)	0.282 (± 0.01)	94.823 (± 27.11)
	LL	13.783 (± 2.43)	0.280 (± 0.01)	48.401 (± 9.53)
SA21	ML	12.995 (± 5.08)	0.214 (± 0.01)	58.994 (± 20.67)
	HL	26.269 (± 1.33)	0.263 (± 0.01)	103.691 (± 11.04)
	LL	24.098 (± 5.39)	0.243 (± 0.01)	107.822 (± 25.50)
SA30	ML	19.043 (± 7.59)	0.217 (± 0.00)	90.613 (± 39.84)
	HL	24.592 (± 1.45)	0.272 (± 0.03)	90.658 (± 8.57)
S	N/A	p = 0.090	p = 0.499	p = 0.095
I	N/A	**p < 0.001**	**p < 0.001**	**p = 0.043**
S × I	N/A	**p = 0.020**	p = 0.208	**p = 0.049**

Discussion

Juvenile sporophytes of *M. pyrifera* responded differently to salinity and irradiance in both growth and photosynthetic performance. The clearest interactive effect was observed for area growth: increasing irradiance enhanced growth at all salinity levels, but the absolute increase from LL to HL was smaller under the lowest salinity (1.65% day^{-1} at SA12) than under the reference salinity (3.35% day^{-1} at SA30), suggesting that hyposalinity constrained the growth response to increased light availability. The hypothesis was therefore partially supported, as this pattern was not consistent across all response

variables. In contrast to growth, photochemical responses were non-monotonic: the lowest F_v/F_m and $rETR_{max}$ values occurred under hyposalinity and intermediate irradiance (SA12–ML), rather than under the lowest irradiance, while α was significantly lower under ML than under LL and HL when averaged across salinity levels. Because the irradiances evaluated were relatively low and representative of turbid or under-canopy environments (Celis-Plá et al. 2021; Le et al. 2022), light likely acted as a limiting resource rather than as a high-light stressor, making photoinhibition an unlikely explanation for this pattern. Although osmotic stress can impair photosynthetic performance in brown macroalgae (Takolander et al. 2017; Morales et al. 2025), it does not readily explain why the lowest values occurred specifically under intermediate irradiance. Moreover, area growth under ML did not differ significantly from HL within any salinity level, indicating that the reduction in photochemical performance was not accompanied by a detectable reduction in growth relative to HL over the experimental period. The mechanism underlying this non-monotonic response remains unclear and warrants further investigation using a broader and more finely resolved irradiance gradient.

This apparent decoupling between growth and photochemical performance may be explained by the fact that fluorescence-based parameters reflect photosynthetic status at the time of measurement, whereas growth integrates physiological responses over longer periods (Román et al. 2020). In this context, reduced growth under hyposalinity could be related to the allocation of resources to adjustments required to maintain osmotic and ionic homeostasis (Fernández et al. 2026). In kelps and other brown macroalgae, exposure to low salinity induces transcriptional and metabolic responses that may increase maintenance costs and reduce the resources available for growth (Takolander et al. 2017; Machado Monteiro et al. 2019; Rugiu et al. 2020). Consistent with this pattern, low salinity reduced growth and mannitol content in *Saccharina latissima* without markedly affecting F_v/F_m (Monteiro et al. 2021), indicating that growth can be constrained even when maximum photochemical efficiency remains relatively stable.

Photosynthetic parameters differed in their responses to salinity and irradiance. While $rETR_{max}$ was significantly affected by irradiance and its interaction with salinity, α showed a significant main effect of irradiance, with generally lower values under intermediate irradiance. E_k was also significantly affected by irradiance and the salinity × irradiance interaction, although Tukey's post hoc comparisons did not detect significant differences between individual treatment pairs. These results suggest that different components of photosynthetic performance responded differently to the experimental conditions. This differential response among components of photosynthetic performance is consistent with the physiological plasticity described for *M. pyrifera* in Magallanes, where populations exposed to contrasting environmental conditions exhibit adjustments in photosynthetic performance and pigment composition (Marambio et al. 2023; Gómez et al. 2025). However, because the sporophytes evaluated originated from a single population, our results represent the response of that population and not necessarily that of the species throughout the region. Considering that early life stages of *M. pyrifera* may respond differently depending on their population of origin and the environmental conditions to which they are exposed (Rodríguez et al. 2019), populations with different histories of exposure to glacial runoff may respond differently to the combined effects of salinity and irradiance.

This dependence on environmental context is particularly relevant in the Magellanic Sub-Antarctic Ecoregion, where freshwater and sediment inputs generate pronounced gradients in salinity,

temperature, and turbidity associated with the degree of glacial influence (Palacios et al. 2021; Bahamonde et al. 2022; Coral-Santacruz et al. 2024). In these environments, decreases in surface salinity often coincide with reduced light availability due to suspended material. In our experiment, the lowest mean growth rates for both area and biomass were recorded under the combination of hyposalinity and low irradiance (SA12–LL), suggesting that simultaneous exposure to these conditions may constrain the development of juvenile sporophytes. Recent studies have documented variation in the physiological performance of *M. pyrifera* along gradients of glacial influence (Marambio et al. 2023; Coral-Santacruz et al. 2024; Rodríguez et al. 2026). Our results complement this evidence by experimentally showing that the response of juvenile sporophytes to irradiance depends on salinity conditions, highlighting the importance of evaluating both factors jointly in these environments.

The sensitivity of juvenile sporophytes to hyposalinity and reduced irradiance may have implications for the recruitment and renewal of *M. pyrifera* forests. Environmental conditions experienced during the early stages of the life cycle can affect germination, development, and subsequent sporophyte formation (Rodríguez et al. 2019). Similarly, exposure of gametophytes to low salinity can reduce their growth and subsequently affect the density and size of embryonic sporophytes (Farmer et al. 2026). Although our study did not evaluate gametophytes or follow individuals through to adult stages, these findings suggest that the effects of hyposalinity may occur at different stages of early development. Because recruitment contributes to the renewal and resilience of kelp forests (Veenhof et al. 2022; Barrientos et al. 2024), monitoring early life stages could provide information on changes in their recovery capacity. This distinction is particularly relevant in high-latitude environments, where the persistence of adult individuals does not necessarily reflect the dynamics of the life stages responsible for population renewal (Pessarrodona et al. 2026). In glacier-influenced coastal environments, characterizing how the early development of *M. pyrifera*, an ecologically and economically important species, responds to salinity and light availability may therefore help anticipate how glacier retreat affects juvenile establishment. Such information may also contribute to the design of cultivation protocols and the identification of potential restoration sites, although its application to management requires validation under field conditions.

Overall, our results show that hyposalinity modifies the response of juvenile *M. pyrifera* sporophytes to light availability in terms of area growth and photosynthetic performance. The combination of hyposalinity and low irradiance primarily constrained growth, whereas the interaction between both factors modified photochemical performance in a non-linear manner. These findings highlight the importance of jointly evaluating environmental factors associated with glacial influence and provide a basis for future research incorporating natural environmental variability, different temperatures, and populations exposed to varying degrees of glacial influence. Further studies could also include analyses of photosynthetic pigments and photoprotective mechanisms to better understand the physiological mechanisms underlying these responses and how environmental changes during early life stages may affect the recruitment, resilience, and renewal capacity of kelp forests in the Magellanic Sub-Antarctic Ecoregion under increasing glacier melt.

Declarations

Funding

This research was supported by FONDECYT Regular project No. 1241697, the Cape Horn International Center (CHIC; ANID BASAL FB210018), and PROASA Project 2025/07548-9.

Competing interests

The authors declare that they have no competing interests.

Availability of data and material

The data supporting the findings of this study are available from the corresponding author upon reasonable request.

Code availability

The R scripts used for data processing, statistical analyses, and graphical representations are available from the corresponding author upon reasonable request.

Authors' contributions

Conceptualization and methodology: CGM, JM, AM. Data collection and analysis: CGM, JPO, FB. Writing – original draft: CGM, JPO. Writing – review and editing: CGM, JM, JPO, FB, JPR, AM.

References

Ávila M, Merino C, Guissen K, Piel MI (2010) Manual de cultivo de macroalgas pardas: desde el laboratorio al océano. Programa de manejo, cultivo y repoblamiento para las algas pardas en la región de Tarapacá. Proyecto FICR–Gobierno Regional de Tarapacá

Bahamonde F, Frangopulos M, Barreiro A, Mafra LL Jr, Jaramillo B, Rodríguez JP, Méndez F, Marambio J, Iriarte JL, Mansilla A (2024) The second skin of macroalgae: unveiling the biodiversity of epiphytic microalgae across environmental gradients of the Magellan Subantarctic ecoregion. Sci Total Environ 956:177229. https://doi.org/10.1016/j.scitotenv.2024.177229

Bahamonde F, Rodríguez JP, Rosenfeld S, Méndez F, López Z, Gerard K, Mansilla A (2022) Variability at multiple spatial scales in intertidal and subtidal macrobenthic communities in a fjord with glaciers, Magellanic Subantarctic ecoregion, Chile. Prog Oceanogr 208:102879. https://doi.org/10.1016/j.pocean.2022.102879

Barrientos S, Piñeiro-Corbeira C, Díaz-Tapia P, García ME, Barreiro R (2024) Recruitment as a possible indicator of declining resilience in degraded kelp forests. Ecol Indic 160:111917. https://doi.org/10.1016/j.ecolind.2024.111917

Celis-Plá PSM, Kappes JL, Figueroa FL, Pereda SV, Villegas K, Altamirano R, Hernández-González MC, Buschmann AH (2021) Solar radiation as an isolated environmental factor in an experimental mesocosm approach for studying photosynthetic acclimation of *Macrocystis pyrifera* (Ochrophyta). Front Plant Sci 12:622150. https://doi.org/10.3389/fpls.2021.622150

Coral-Santacruz D, Méndez F, Marambio J, Haye PA, Bahamonde F, Mansilla A (2024) Effects of glacial melting on physiological performance of *Macrocystis pyrifera* in the Fjord of the Mountains, Magellanic Sub-Antarctic ecoregion, Chile. J Appl Phycol 36:3637–3648. https://doi.org/10.1007/s10811-024-03362-3

Dussaillant I, Berthier E, Brun F, Masiokas M, Hugonnet R, Favier V, Rabatel A, Pitte P, Ruiz L (2019) Two decades of glacier mass loss along the Andes. Nat Geosci 12:802–808. https://doi.org/10.1038/s41561-019-0432-5

Farmer C, Pereda SV, Villegas K, Hernández-González MC, Buschmann AH (2026) Effect of low salinity on the microscopic stages of *Macrocystis pyrifera*: an experimental approach for explaining changes in population dynamics on annual populations. Research Square [Preprint]. https://doi.org/10.21203/rs.3.rs-8713868/v1

Fernández PA, Poza AM, Wallet T, Hernández X, Camus C (2026) Ecotypic differentiation in populations of the giant kelp *Macrocystis pyrifera* from southern Chile: implications for the species aquaculture development. Algal Res 95:104633. https://doi.org/10.1016/j.algal.2026.104633

Frangopulos M, Bahamonde F, Johnson E, Alarcón C, Cárdenas C, Toro C, Salgado P, Mansilla A, Pizarro G, Iriarte JL (2026) Environmental drivers determined by remote sensing and in-situ measurements during a spring phytoplankton bloom event in the fjords and channels of southern Chile. ISPRS Ann Photogramm Remote Sens Spatial Inf Sci X-3/W4-2025:141–147. https://doi.org/10.5194/isprs-annals-X-3-W4-2025-141-2026

Gómez I, Loaiza J, Palacios M, Osman D, Huovinen P (2025) Functionality of photobiological traits of the giant kelp (*Macrocystis pyrifera*) as key determinant to thrive in contrasting habitats in a sub-Antarctic region. Sci Total Environ 971:179055. https://doi.org/10.1016/j.scitotenv.2025.179055

Gonzalez-Aragon D, Rivadeneira MM, Lara C, Torres FI, Vásquez JA, Broitman BR (2024) A species distribution model of the giant kelp *Macrocystis pyrifera*: worldwide changes and a focus on the Southeast Pacific. Ecol Evol 14:10901. https://doi.org/10.1002/ece3.10901

Le DM, Desmond MJ, Buschmann AH, Pritchard DW, Camus C, Hurd CL, Hepburn CD (2022) Reproduction, hatchery and culture applications for the giant kelp (*Macrocystis pyrifera*): a methodological appraisal. Applied Phycology 3:368–382. https://doi.org/10.1080/26388081.2022.2086823

Lebrun A, Miller CA, Meynadier M, Comeau S, Urrutti P, Alliouane S, Schlegel R, Gattuso JP, Gazeau F (2024) Multifactorial effects of warming, low irradiance, and low salinity on Arctic kelps. Biogeosciences 21:4605–4620. https://doi.org/10.5194/bg-21-4605-2024

Machado Monteiro CM, Li H, Bischof K, Bartsch I, Valentin KU, Corre E, Collén J, Harms L, Glöckner G, Heinrich S (2019) Is geographical variation driving the transcriptomic responses to multiple stressors in the kelp *Saccharina latissima*? BMC Plant Biol 19:513. https://doi.org/10.1186/s12870-019-2124-0

Marambio J, Diehl N, Bischof K (2022a) High ecophysiological plasticity of *Desmarestia aculeata* (Phaeophyceae) present in an Arctic fjord under varying salinity and irradiance conditions. Biology (Basel) 11:1499. https://doi.org/10.3390/biology11101499

Marambio J, Rodríguez JP, Méndez F, Ocaranza P, Rosenfeld S, Ojeda J, Rautenberger R, Bischof K, Terrados J, Mansilla A (2017) Photosynthetic performance and pigment composition of *Macrocystis pyrifera* (Laminariales, Phaeophyceae) along a gradient of depth and seasonality in the ecoregion of Magellan, Chile. J Appl Phycol 29:2575–2585. https://doi.org/10.1007/s10811-017-1136-0

Marambio J, Rodríguez JP, Rosenfeld S, Méndez F, Ojeda J, Ocaranza P, Bischof K, Mansilla A (2023) New ecophysiological perspectives on the kelp *Macrocystis pyrifera*: generating a basis for sustainability in the sub-Antarctic region. Front Mar Sci 10:1222178. https://doi.org/10.3389/fmars.2023.1222178

Marambio J, Rosenfeld S, Bischof K (2022b) Hyposalinity affects diurnal photoacclimation patterns in the rhodophyte *Palmaria palmata* under mimicked Arctic summer conditions. J Photochem Photobiol 11:100124. https://doi.org/10.1016/j.jpap.2022.100124

McLachlan J (1973) Growth media—marine. In: Stein JR (ed) Handbook of phycological methods: culture methods and growth measurements. Cambridge University Press, Cambridge, pp 25–51

Monteiro C, Li H, Diehl N, Collén J, Heinrich S, Bischof K, Bartsch I (2021) Modulation of physiological performance by temperature and salinity in the sugar kelp *Saccharina latissima*. Phycol Res 69:48–57. https://doi.org/10.1111/pre.12443

Morales F, Muñoz PT, Undabarrena A, Celis-Plá PSM, Rámila C, Aguilar-Muñoz P, Molina V, Navarro NP, Sáez CA, Lavergne C, Cámara B, Tessini C, González-Pino K, Pérez-Hernández GB, Rodríguez-Rojas F (2025) Climate change-related salinity fluctuations and warming induce physiological stress and cellular alterations in an Antarctic intertidal brown alga. Environments 12:390. https://doi.org/10.3390/environments12100390

Ojeda J, Catalán C, Marambio J, Rosenfeld S, Rodríguez JP, Cuevas M, Mansilla A (2026) Kelp forest as critical habitat: evidence gaps and ecosystem-based governance across Sub-Antarctic channel–fjord systems. Curr Opin Environ Sustain 83:101728. https://doi.org/10.1016/j.cosust.2026.101728

Palacios M, Osman D, Ramírez J, Huovinen P, Gómez I (2021) Photobiology of the giant kelp *Macrocystis pyrifera* in the land-terminating glacier fjord Yendegaia (Tierra del Fuego): a look into the future? Sci Total Environ 751:141810. https://doi.org/10.1016/j.scitotenv.2020.141810

Pessarrodona A, Palacios M, Kaminsky J, Mora-Soto A, Dayton PK, Hüne M (2026) Footprints of global change in Patagonian kelp forests after half a century. Reg Environ Change 26:194. https://doi.org/10.1007/s10113-026-02680-1

Platt T, Gallegos CL, Harrison WG (1980) Photoinhibition of photosynthesis in natural assemblages of marine phytoplankton. J Mar Res 38:687–701

R Core Team (2022) R: a language and environment for statistical computing. R Foundation for Statistical Computing, Vienna. https://www.R-project.org/

Rivera A, Aravena JC, Urra A, Reid B (2023) Chilean Patagonian glaciers and environmental change. In: Castilla JC, Armesto Zamudio JJ, Martínez-Harms MJ, Tecklin D (eds) Conservation in Chilean Patagonia. Integrated Science, vol 19. Springer, Cham, pp 393–407. https://doi.org/10.1007/978-3-031-39408-9_15

Rodríguez JP, Mansilla A, Martínez-Cruz K, López-Farrán Z, Marambio J, Bahamonde F, Méndez F (2026) Environmental history shapes ecophysiology and microbiota of *Macrocystis pyrifera* at contrasting glacier- and ocean-influenced sites in the Magellanic sub-Antarctic ecoregion. Front Conserv Sci 7:1873259. https://doi.org/10.3389/fcosc.2026.1873259

Rodríguez JP, Terrados J, Rosenfeld S, Méndez F, Ojeda J, Mansilla A (2019) Effects of temperature and salinity on the reproductive phases of *Macrocystis pyrifera* (L.) C. Agardh (Phaeophyceae) in the Magellan region. J Appl Phycol 31:915–928. https://doi.org/10.1007/s10811-018-1693-x

Román M, Román S, Vázquez E, Troncoso J, Olabarria C (2020) Heatwaves during low tide are critical for the physiological performance of intertidal macroalgae under global warming scenarios. Sci Rep 10:21408. https://doi.org/10.1038/s41598-020-78526-5

Rosenfeld S, Maturana CS, Gañan M, Rendoll Cárcamo J, Díaz A, Contador T, Aldea C, Gonzalez-Wevar C, Orlando J, Poulin E (2023) Revealing the hidden biodiversity of Antarctic and the Magellanic Sub-Antarctic Ecoregion: a comprehensive study of aquatic invertebrates from the BASE Project. Biodivers Data J 11:108566. https://doi.org/10.3897/BDJ.11.e108566

Rozzi R, Armesto JJ, Gutiérrez JR, Massardo F, Likens GE, Anderson CB, Poole A, Moses KP, Hargrove E, Mansilla AO, Kennedy JH, Willson M, Jax K, Jones CG, Callicott JB, Arroyo MTK (2012) Integrating ecology and environmental ethics: earth stewardship in the southern end of the Americas. BioScience 62:226–236. https://doi.org/10.1525/bio.2012.62.3.4

Rugiu L, Panova M, Pereyra RT, Jormalainen V (2020) Gene regulatory response to hyposalinity in the brown seaweed *Fucus vesiculosus*. BMC Genomics 21:42. https://doi.org/10.1186/s12864-020-6470-y

Takolander A, Leskinen E, Cabeza M (2017) Synergistic effects of extreme temperature and low salinity on foundational macroalga *Fucus vesiculosus* in the northern Baltic Sea. J Exp Mar Biol Ecol 495:110–118. https://doi.org/10.1016/j.jembe.2017.07.001

Valdenegro A, Silva N (2003) Caracterización oceanográfica física y química de la zona de canales y fiordos australes de Chile entre el estrecho de Magallanes y cabo de Hornos (CIMAR 3 Fiordos). Ciencia y Tecnología del Mar 26:19–60

Veenhof RJ, Champion C, Dworjanyn SA, Wernberg T, Minne AJP, Layton C, Bolton JJ, Reed DC, Coleman MA (2022) Kelp gametophytes in changing oceans. In: Hawkins SJ, Lemasson AJ, Allcock AL, Bates AE, Byrne M, Evans AJ, Firth LB, Lucas CH, Marzinelli EM, Mumby PJ, Russell BD,

549 Sharples J, Smith IP, Swearer SE, Todd PA (eds) Oceanography and marine biology: an annual review,
550 vol 60. CRC Press, Boca Raton, pp 335–372. https://doi.org/10.1201/9781003288602-7

551 Yong YS, Yong WTL, Anton A (2013) Analysis of formulae for determination of seaweed growth
552 rate. J Appl Phycol 25:1831–1834. https://doi.org/10.1007/s10811-013-0022-7

Supplementary Files

This is a list of supplementary files associated with this preprint. Click to download.

- CGM.pdf